

# STRelay: A Universal Spatio-Temporal Relaying Framework for Location Prediction with Future Spatiotemporal Contexts

Bangchao Deng<sup>1</sup>, Lianhua Ji<sup>1</sup>, Chunhua Chen<sup>1</sup>, Xin Jing<sup>1</sup>, Ling Ding<sup>1</sup>,  
Bingqing QU<sup>2</sup>, Pengyang Wang<sup>1</sup>, Dingqi Yang<sup>1\*</sup>

<sup>1</sup>The State Key Laboratory of Internet of Things for Smart City, University of Macau, China

<sup>2</sup>Beijing Normal University-Hong Kong Baptist University United International College  
{yc37980, mc45079, chunhuachen, yc27431, mc36510, pengyangwang, dingqiyang}@um.edu.mo, bingqingqu@uic.edu.cn

## Abstract

Next location prediction is a critical task in human mobility modeling, enabling applications like travel planning and urban mobility management. Existing methods mainly rely on historical spatiotemporal trajectory data to train sequence models that directly forecast future locations. However, they often overlook the importance of the future spatiotemporal contexts, which are highly informative for the future locations. For example, knowing how much time and distance a user will travel could serve as a critical clue for predicting the user’s next location. Against this background, we propose **STRelay**, a universal **S**patio**T**emporal **R**elaying framework explicitly modeling the future spatiotemporal context given a human trajectory, to boost the performance of different location prediction models. Specifically, STRelay models future spatiotemporal contexts in a relaying manner, which is subsequently integrated with the encoded historical representation from a base location prediction model, enabling multi-task learning by simultaneously predicting the next time interval, next moving distance interval, and finally the next location. We evaluate STRelay integrated with four state-of-the-art location prediction base models on four real-world trajectory datasets. Results demonstrate that STRelay consistently improves prediction performance across all cases by 3.19%-11.56%. Additionally, we find that the future spatiotemporal contexts are particularly helpful for entertainment-related locations and also for user groups who prefer traveling longer distances. The performance gain on such non-daily-routine activities, which often suffer from higher uncertainty, is indeed complementary to the base location prediction models that often excel at modeling regular daily routine patterns.

## Introduction

With the rapid growth of location-based social media, users are increasingly inclined to share their activities on Location-Based Social Networks (LBSNs), generating rich digital footprints for human mobility studies (Yang et al. 2014). A key task in human mobility modeling is predicting a user’s next location based on the user’s historical mobility trajectory (Noulas et al. 2012), which is a fundamental building block supporting various location-based applications, such as travel planning (Zhou et al. 2021), taxi ride-sharing scheduling (Ma, Zheng, and Wolfson 2013), and user behavior patterns analyzing (Sun et al. 2020).

\*Corresponding author

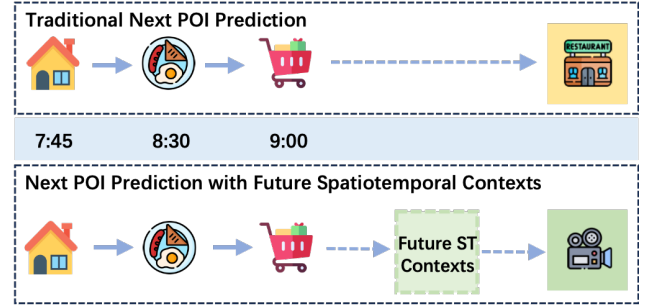


Figure 1: Examples of two prediction paradigms. Paradigm 1 (top): Predict the same POI given historical data of a user. Paradigm 2 (Bottom): Considering future time and moving distance, predict different POIs based on future spatiotemporal contexts.

To leverage the spatiotemporal characteristics of trajectory data, various methods have been proposed for next Point of Interest (POI) prediction<sup>1</sup>. Traditional next POI prediction methods forecast future locations relying solely on historical spatiotemporal information. For example, sequential transitions are typically captured using Markov chain models (Rendle, Freudenthaler, and Schmidt-Thieme 2010; Cheng et al. 2013; Feng et al. 2015), while long-term dependencies are modeled through RNNs (Liu et al. 2016; Zhao et al. 2019) and attention-based architectures (Lian et al. 2020). More recently, some methods using additional context, such as historical spatiotemporal contexts (Yang et al. 2020) and social networks (Rao et al. 2022; Qin et al. 2023; Xu et al. 2023), have been proposed for further performance improvement. *However, these methods overlook the time information of the predicted next location, and thus always make the same prediction given a historical trajectory.* Some recent approaches have utilized predicted (or even actual) future temporal information to enhance location prediction, effectively capturing time-specific user behaviors. For example, some methods explicitly incorporate future timestamps as query inputs to model time-dependent mobility patterns (Feng et al. 2024; Deng et al. 2025b). Alternatively,

<sup>1</sup>Given the context of human trajectories, we do not distinguish the two terms “location” and “POI” throughout this paper.

other techniques (Yang, Liu, and Zhao 2022; Song, Ren, and Lu 2025) jointly optimize timestamp prediction and location forecasting through integrated temporal modeling to improve predictive accuracy. *However, there still lacks systematic studies on the key role of future spatiotemporal contexts in location prediction, which, as we show in this paper, are highly informative for the future locations.* For example, knowing how much time and distance a user will travel could serve as a strong indicator for forecasting the user’s next location.

Against this background, we propose a novel prediction paradigm by first learning to predict the future spatiotemporal contexts, which are then fed as additional inputs to a base location prediction model to boost the location prediction performance. This paradigm has the following two-fold advantages. On one hand, human mobility patterns exhibit inherent heterogeneity. For instance, entertainment activities and daily routines (e.g., home-workplace commuting) demonstrate distinct spatiotemporal patterns: the former often exhibits more variable spatiotemporal distributions, while the latter tends to be less variable. By modeling future spatiotemporal contexts, we can effectively accommodate such heterogeneity, in particular, benefiting the more variable entertainment activities, where traditional sequence models often fail (as evidenced by our experiments later). On the other hand, the spatiotemporal preferences of users also exhibit different characteristics. For example, two users might have the same lunch schedule, but their travel preferences differ: a convenience-oriented user may take 10 minutes to go to nearby places like an office cafeteria within 500m; in contrast, an adventurous user may be willing to spend half an hour traveling 5 km to go to a fancy restaurant. Subsequently, modeling the future spatiotemporal contexts of users can effectively benefit such a scenario. Our empirical analysis also shows that incorporating the future spatiotemporal contexts can significantly reduce mobility entropy (Zhang, Zhao, and Chen 2022; Sun et al. 2024), thereby showing great potential to improve the predictability of the next location (see Figure 2 in Section Empirical Analysis on Future Spatiotemporal Contexts for details).

Motivated by the above observations, we propose **STRelay**, a universal **S**patio**T**emporal **R**elaying framework that explicitly learns to model the future spatiotemporal contexts given a human trajectory, to boost the performance of different location prediction models. Specifically, we first define the future spatiotemporal contexts as the elapsed time and distance from the present location to the next location in a trajectory, and then discretize them into temporal and spatial intervals under a predefined granularity (1 hour for time or 1 km for distance, respectively). Our objective is to predict the future temporal and spatial intervals based on user trajectories. To capture the inherent relationship between the temporal and spatial contexts, STRelay first learns user- and timestamp-specific representations to query all temporal intervals to obtain a temporal context representation, and subsequently queries all spatial intervals conditioned on the temporal context representation to output a spatial context representation, in a relaying manner. Afterwards, a base location prediction model is used to encode the past trajectory

information, which is concatenated with our temporal and spatial context representations to predict the next location. Additionally, to ensure the quality of the learnt future spatiotemporal contexts, we provide supervision signals to the temporal and spatial intervals in the training process under a multi-task learning scheme, where we optimize not only for the prediction of the next location, but also the prediction of the future temporal and spatial intervals.

Our contributions can be summarized as follows:

- We reveal the importance of future spatiotemporal contexts for next location prediction tasks, serving as a strong indicator for improving the predictability of the next location.
- We propose STRelay, a universal framework designed to explicitly model the future spatiotemporal contexts in a relaying manner; it can be flexibly integrated with different location prediction models under encoder-decoder architectures to boost the prediction performance.
- We evaluate STRelay integrated with four state-of-the-art location prediction base models on four real-world trajectory datasets. Results demonstrate that STRelay consistently improves prediction performance across all cases by 3.19%-11.56%. Additionally, we find that the future spatiotemporal contexts are particularly helpful for entertainment-related locations and also for user groups who prefer traveling longer distances, which is indeed complementary to the base location prediction models that often excel at modeling daily routine patterns.

## Related Work

Location prediction is a key problem in human mobility modeling, aiming to predict a user’s future location based on their historical mobility trajectories. Traditional next POI prediction methods focus on learning mobility patterns from user historical trajectories. Early approaches relied on features such as location visit frequency (Noulas et al. 2012) or activity preferences. Markov chain-based models (Rendle, Freudenthaler, and Schmidt-Thieme 2010; Cheng et al. 2013; Feng et al. 2015) capture sequential transitions between locations, while recurrent neural network (RNN)-based models (Liu et al. 2016; Zhao et al. 2019) and attention-based models (Lian et al. 2020) effectively model long-term dependencies in mobility trajectories. The Flashback mechanism (Yang et al. 2020) enhances prediction accuracy by leveraging historical hidden states with similar spatiotemporal contexts, inspiring subsequent works (Cao et al. 2021; Li et al. 2021; Wu et al. 2022; Liu et al. 2022; Rao et al. 2022). Additionally, Graph Neural Networks (GNNs) have been employed to enrich representations by constructing spatiotemporal transition graphs (Rao et al. 2022; Yin et al. 2023), historical distance graphs (Qin et al. 2023), or user preference graphs (Xu et al. 2023). However, these methods typically produce static predictions for all future times based on a given mobility trace, limiting their adaptability to dynamic real-world scenarios. Furthermore, several methods incorporate predicted or even actual future temporal information to guide location predictions, capturing time-specific user behaviors. For example, they

utilize future timestamps as query timestamps (Gao, Tang, and Liu 2012; Yang et al. 2019; Li et al. 2021; Feng et al. 2024; Deng et al. 2025b) or a query time interval (Zhao et al. 2019, 2020; Feng et al. 2018) to predict a user’s location after a specified period. Others employ a fixed query time threshold to forecast locations within an upcoming time window (Feng et al. 2015, 2018). An alternative approach integrates timestamp prediction with location forecasting to improve predictive accuracy (Yang, Liu, and Zhao 2022; Sun et al. 2024; Song, Ren, and Lu 2025). However, there still lacks systematic studies on the key role of future spatiotemporal contexts in location prediction, which, as we show in this paper, are highly informative for the future locations.

Against this background, we propose STRelay, a universal framework that learns to model the future spatiotemporal contexts given a human trajectory, to boost the performance of different location prediction models.

## Preliminaries

In this section, we introduce several preliminaries, including the problem definition and empirical data analyses supporting our motivation.

### Problem Definition

**Human Trajectory.** A trajectory is a time-ordered sequence  $X = \{x_1, x_2, \dots, x_n\}$ , where each event (check-in)  $x_i = (u, t_i, l_i)$  represents a presence event of a user  $u$ , with  $t_i$  denoting the event time and  $l_i$  indicating the location (POI) with its geographic coordinates.

**Next Location Prediction.** Given a user’s historical trajectory  $X = \{x_1, x_2, \dots, x_n\}$ , the task aims to predict the most likely POI  $l_{n+1}$  that the user will visit in the next check-in event  $x_{n+1}$ .

### Empirical Analysis on Future Spatiotemporal Contexts

We conduct an empirical analysis from the perspective of mobility entropy to reveal the importance of the future spatiotemporal context for next location prediction. Specifically, we first focus solely on the trajectory sequence and compute the mobility entropy (Zhang, Zhao, and Chen 2022) for each user as follows:

$$E(S^u) = - \sum_{i=1}^{N^u} p(l_i) \log_2 p(l_i) \quad (1)$$

where  $S^u$  represents the trajectory sequence of user  $u$ ,  $N^u$  denotes the number of unique locations visited by  $u$  in  $S^u$ , and  $p(l_i)$  denotes the frequency of location  $l_i$  occurring in  $S^u$ .

Furthermore, we introduce future temporal context into the mobility entropy through categorizing locations visited by users into their respective future  $t$ , and then compute the mean mobility entropy after accounting for future temporal context as follows:

$$E^t(S^u) = - \frac{1}{N^t} \sum_{t=1}^{N^t} \sum_{i=1}^{N_t^u} p(l_i, t) \log_2 p(l_i, t) \quad (2)$$

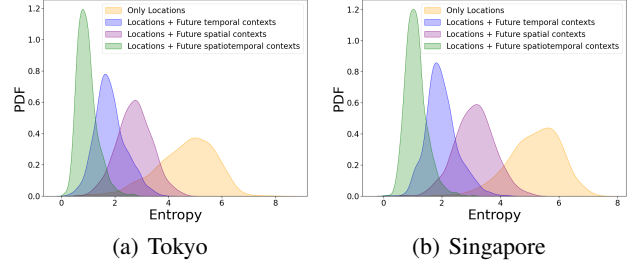


Figure 2: Influence of spatiotemporal contexts on mobility entropy

where  $N^t$  represents the number of  $t$ ,  $N_t^u$  is the count of unique locations visited by user  $u$  with  $t$ , and  $p(l_i, t)$  denotes the frequency of location  $l_i$  appearing with  $t$ .

Similarly, we introduce future spatial context into the mobility entropy through categorizing locations visited by users into their respective future moving distance  $d$ , and then compute the mean mobility entropy after accounting for future spatial context as follows:

$$E^s(S^u) = - \frac{1}{N^d} \sum_{d=1}^{N^d} \sum_{i=1}^{N_d^u} p(l_i, d) \log_2 p(l_i, d) \quad (3)$$

where  $N^d$  represents the number of  $d$ ,  $N_d^u$  is the count of unique locations visited by user  $u$  with  $d$ , and  $p(l_i, d)$  denotes the frequency of location  $l_i$  appearing with  $d$ .

In the end, we further consider both spatial and temporal contexts to get mobility entropy with the future spatiotemporal contexts:

$$E^{st}(S^u) = - \frac{1}{N^t} \frac{1}{N^d} \sum_{t=1}^{N^t} \sum_{d=1}^{N^d} \sum_{i=1}^{N_{td}^u} p(l_i, t, d) \log_2 p(l_i, t, d) \quad (4)$$

where  $N^d$  represents the number of distance intervals,  $N_{td}^u$  is the count of unique locations visited by user  $u$  with  $t$  in  $d$ , and  $p(l_i, t, d)$  denotes the frequency of location  $l_i$  appearing with  $t$  in  $d$ .

The distributions of the mobility entropy on our Tokyo and Singapore datasets (more details below) are shown in Figure 2. We observe that the introduction of temporal context or spatial context can effectively reduce mobility entropy in both datasets. This reduction suggests that involving future spatiotemporal contexts for next location prediction has great potential to reduce the uncertainty of the next location, ultimately resulting in higher predictability.

## STRelay

The framework of our STRelay is shown in Figure 3. First, to model future spatiotemporal contexts to boost the performance, we discretize spatiotemporal contexts into temporal and spatial intervals under a predefined granularity. Then, we capture the inherent relationship between temporal and spatial contexts by first learning to model temporal context representations, and subsequently conditioning on the temporal context representation to output a spatial context rep-

resentation. Afterward, we encode historical latent representation from a base location prediction model, along with our spatial and temporal context representations, and feed them into a multi-task prediction layer, simultaneously predicting the next time interval, next moving distance interval, and finally the next location. In the following, we elaborate on our model design, followed by the training process.

### Future Spatiotemporal Context Modeling

In this paper, we define the future spatiotemporal contexts as the elapsed time and distance from a user's current location to their next location in a trajectory. By effectively modeling how much time the user will spend traveling and how far the user will go, such spatiotemporal contexts serve as critical predictive features for next location forecasting, providing deeper insights into users' forthcoming mobility patterns, thereby enhancing location prediction performance.

**Discretization of Future Spatiotemporal Contexts.** The future spatiotemporal contexts are inherently continuous and dynamic; we first discretize them into temporal and spatial intervals under a predefined granularity.

For temporal intervals, we define a minimum interval  $\Delta t$  (e.g., 1 hour) and a maximum interval  $M\Delta t$  (e.g., 24 hours), constructing a discrete candidate set:

$$\mathcal{T} = \{\Delta t, 2\Delta t, \dots, M\Delta t\} \quad (5)$$

Noted that any interval exceeding  $M\Delta t$  is capped at  $M\Delta t$ . Each temporal interval between consecutive check-ins is assigned to its corresponding bin and represented as an  $M$ -dimensional one-hot vector  $\tau \in \mathbb{R}^M$ .

Similarly, for spatial intervals, we define a minimum interval  $\Delta d$  (e.g., 1 km) and a maximum interval  $N\Delta d$  (e.g., 30 km), forming a discrete candidate set:

$$\mathcal{D} = \{\Delta d, 2\Delta d, \dots, N\Delta d\} \quad (6)$$

where any distances exceeding  $N\Delta d$  are capped at  $M\Delta t$ , and each future spatial distance between consecutive check-ins is assigned to its corresponding bin and represented as an  $N$ -dimensional one-hot vector  $\rho \in \mathbb{R}^N$ . Afterwards, for all candidate future temporal and spatial intervals, we embed them into a latent space as learnable embeddings  $E^T \in \mathbb{R}^{M \times d}$  and  $E^D \in \mathbb{R}^{N \times d}$ , respectively, where  $d$  is the dimension of the embedding space.

These discretization and embedding approaches enhance training stability by reducing sensitivity to minor variations (e.g., treating 6 hours and 6.17 hours, or 8 km and 8.3 km as the same intervals since they share similar properties), enabling robust modeling of temporal and spatial context representations for next POI prediction. We also conduct experiments to investigate the impact of different temporal and spatial granularities in our experiments later.

### Representation of Future Spatiotemporal Contexts.

Human mobility exhibits strong spatiotemporal coupling, where daily routines (e.g., home-work commutes) typically involve both short time intervals and moving distances, while entertainment activities often exhibit longer travel

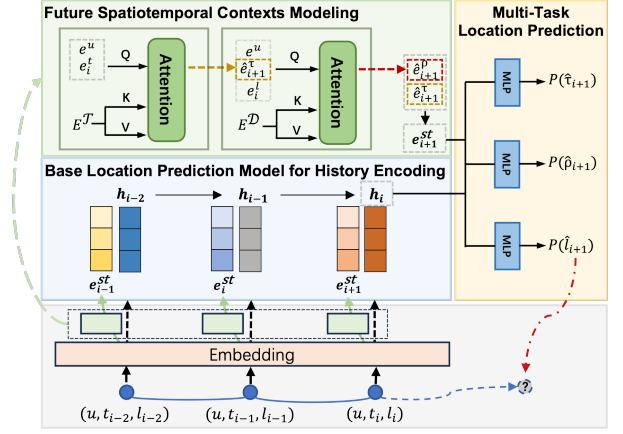


Figure 3: Our proposed STRelay consists of 1) a future spatiotemporal contexts modeling module, 2) a base location prediction model for history encoding, and 3) a multi-task prediction module.

times and distances. To capture such inherent spatiotemporal correlation, we adopt a relaying manner that generates future spatiotemporal context representations by mimicking an individual's sequential decisions about how much time and how far to move next (Yuan et al. 2022; Deng et al. 2025a). Specifically, we first learn a temporal context representation and subsequently condition on the learnt temporal context representation to output a spatial context representation.

Intuitively, the temporal context for the next check-in depends on the user and the current time. For example, a user at a workplace on a weekday morning may check in at a nearby café within 1 hour, while the same user at a park on a weekend may check in at a distant restaurant after 5 hours. To capture this dependency, when predicting next location  $l_{i+1}$ , we first embed the user  $u$  into the low-dimensional embedding space, denoted as  $e^u \in \mathbb{R}^d$ . Next, for the current timestamp  $t_i$ , we convert it to an hour-in-week representation (Deng et al. 2025b) and embed it into a latent space as a learnable embedding  $e_i^t \in \mathbb{R}^d$ , which can naturally capture temporal regularities between weekdays and weekends. Then, we concatenate them to get the temporal query embedding  $e_i^\tau$  for predicting future temporal context:

$$e_i^\tau = [e^u; e_i^t] \quad (7)$$

Then, we use temporal query embedding to query all of the candidate temporal interval embeddings  $E^T$  via an attention mechanism (Vaswani et al. 2017), producing a future temporal context representation  $\hat{e}_{i+1}^\tau$ :

$$Q = e_i^\tau W_Q; K = E^T W_K; V = E^T W_V \quad (8)$$

$$\hat{e}_{i+1}^\tau = \text{softmax} \left( \frac{QK^T}{\sqrt{d_k}} \right) V \quad (9)$$

where  $W_Q$ ,  $W_K$ , and  $W_V$  are the learnable linear projection matrices to map the input into a corresponding subspace.

After obtaining the future temporal representation, we now turn to modeling the spatial dimension. Generally, how

far a user will travel next is influenced by her personal preference, the anticipated timing (i.e., the future temporal representation), and the current location information. To encode these spatiotemporal dependencies and model the future spatial context, we construct a spatial query embedding  $e_i^p$  by concatenating three components: the user embedding  $e^u$ , the future temporal representation  $\hat{e}_{i+1}^t$ , and the latent embedding of the current location  $e_i^l \in \mathbb{R}^d$ , formulated as:

$$e_i^p = [e^u; \hat{e}_{i+1}^t; e_i^l] \quad (10)$$

Afterwards, we get future spatial context representation in a similar way to the temporal aspect as shown in Eq. 8 and Eq. 9. Specifically, we use spatial query embedding  $e_i^p$  as query and  $E^D$  as key and value to produce a weighted future spatial representation  $\hat{e}_{i+1}^p$  by an attention mechanism.

To this end, we concatenate the future temporal context representation  $\hat{e}_{i+1}^t$  and future spatial context representation  $\hat{e}_{i+1}^p$  to obtain the future spatiotemporal context representations  $e_{i+1}^{st}$ .

## History Encoding and Location Prediction

**Base Location Prediction Model for History Encoding.** Our STRelay framework is designed to flexibly integrate with different location prediction models under encoder-decoder architectures. While  $e_{i+1}^{st}$  captures the future temporal and spatial contexts, to predict the next POI  $l_{i+1}$ , we also need to encode historical trajectory information. Given a base location prediction model  $g$ , we input the historical trajectory  $X$  to obtain  $h_i \in \mathbb{R}^d$ , which encodes the historical sequential spatiotemporal information until  $t_i$ :

$$h_i = g(X) \quad (11)$$

Subsequently, we concatenate the hidden state of the trajectory history  $h_i$  and the predicted future spatiotemporal context representation  $e_{i+1}^{st}$  as the overall context embedding  $e^c$ , which integrates both historical and future spatiotemporal contexts for prediction:

$$e^c = [h_i; e_{i+1}^{st}] \quad (12)$$

**Multi-Task Location Prediction.** After the overall context embedding is generated, it is then fed into a multi-layer perceptron (MLP) followed by a softmax function to predict the next location:

$$P(\hat{l}_{i+1}) = \text{softmax}(MLP_\theta(e^c)) \quad (13)$$

where  $\hat{l}_{i+1}$  is the predicted probability distributions for next location.

Meanwhile, to ensure the quality of the learnt future spatiotemporal contexts, we provide supervision signals to the temporal and spatial intervals in the training process under a multi-task learning scheme alongside the POI prediction, using the context embedding  $e^c$ . We define two prediction heads to estimate the probability distributions of future temporal and spatial intervals:

$$P(\hat{\tau}_{i+1}) = \text{softmax}(MLP_\gamma(e^c)), \quad (14)$$

$$P(\hat{\rho}_{i+1}) = \text{softmax}(MLP_\phi(e^c)) \quad (15)$$

where  $\hat{\tau}_{i+1}$  and  $\hat{\rho}_{i+1}$  are the predicted probability distributions for the future temporal and spatial intervals, respectively.

Table 1: Datasets Statistics

Dataset	#Users	#POIs	#Check-ins
Istanbul	8,750	13,194	1,530,050
Tokyo	2,484	8,196	735,211
Singapore	1,164	10,859	281,039
Moscow	2,665	12,527	516,355

## Model Training

The training objective of STRelay can be decomposed into a base location prediction loss and two future spatiotemporal context losses. First, the base historical modeling loss aims to predict the next location:

$$\mathcal{L}_{\text{POI}} = - \sum_{j=1}^U \sum_{i=1}^{N_j-1} l_{i+1,j} \log(P(\hat{l}_{i+1,j})) \quad (16)$$

where  $U$  is the number of users;  $N_j$  is the sequence length of  $j$ -th user;  $l_{i+1,j}$  is the one-hot vector of ground truth POI for  $(i+1)$ -th check-in of  $j$ -th user.

Since both temporal and spatial contexts are discretized, their losses also take the form of a multi-class classification loss. We get the loss of predicting future temporal and spatial contexts as follows:

$$\mathcal{L}_\tau = - \sum_{j=1}^U \sum_{i=1}^{N_j-1} \tau_{i+1,j} \log(P(\hat{\tau}_{i+1,j})) \quad (17)$$

$$\mathcal{L}_\rho = - \sum_{j=1}^U \sum_{i=1}^{N_j-1} \rho_{i+1,j} \log(P(\hat{\rho}_{i+1,j})) \quad (18)$$

The overall loss function of our STRelay combines the three losses as follows:

$$\mathcal{L} = \mathcal{L}_{\text{POI}} + \mathcal{L}_\tau + \mathcal{L}_\rho \quad (19)$$

## Experiments

### Experiment Setup

**Dataset.** We evaluate our STRelay using four widely used real-world datasets: Istanbul, Tokyo, Singapore and Moscow. They are collected from April 2012 to February 2013 (Yang et al. 2019). Each check-in consists of the user ID, POI ID, latitude, longitude, and timestamp. We follow the data pre-processing steps in (Yang et al. 2020). The initial 80% of the data (in chronological order) is used for training, and the remaining data for testing. Table 1 summarizes the details of the four processed datasets.

**Baselines.** We choose the following models for next location prediction as baselines: **BPR** (Rendle et al. 2012), **Caser** (Tang and Wang 2018), **STGN** (Zhao et al. 2019), **STGCN** (Zhao et al. 2019), **DeepMove** (Feng et al. 2018), **STAN** (Luo, Liu, and Liu 2021), **GETNext** (Yang, Liu, and Zhao 2022), **Flashback** (Yang et al. 2020), **SNPM** (Yin et al. 2023), and **Graph-Flashback** (Rao et al. 2022). Please refer to Appendix for the details of baselines.

Among these baselines, we instantiate our STRelay with four techniques: STGN, Flashback, SNPM, and Graph-Flashback to validate its effectiveness.



Table 2: Overall location prediction performance

Methods	Istanbul			Tokyo			Singapore			Moscow		
	Acc@10	NDCG@10	MRR	Acc@10	NDCG@10	MRR	Acc@10	NDCG@10	MRR	Acc@10	NDCG@10	MRR
BPR	0.3816	0.2500	0.1528	0.3215	0.2121	0.1317	0.3193	0.2069	0.1176	0.2093	0.1273	0.0820
Caser	0.3751	0.2649	0.2396	0.5000	0.3275	0.2830	0.3091	0.1953	0.1600	0.3974	0.2579	0.2301
STGCN	0.3949	0.2721	0.2428	0.5306	0.3422	0.2927	0.3691	0.2353	0.2138	0.4237	0.2810	0.2437
DeepMove	0.3368	0.2141	0.1859	0.5107	0.3338	0.2884	0.3871	0.2360	0.2009	0.3790	0.2322	0.1967
STAN	0.3716	0.2467	0.2171	0.4890	0.3147	0.2702	0.3855	0.2382	0.2040	0.3993	0.2474	0.2102
GETNext	0.3816	0.2536	0.2230	0.5197	0.3408	0.2948	0.4008	0.2564	0.2217	0.4302	0.2831	0.2456
STGN	0.3936	0.2704	0.2410	0.5342	0.3529	0.3056	0.3538	0.2209	0.1905	0.4157	0.2755	0.2392
Flashback	0.4139	0.2847	0.2557	0.5459	0.3640	0.3119	0.3815	0.2425	0.2092	0.4410	0.3007	0.2633
SNPM	0.4125	0.2849	0.2527	0.5470	0.3607	0.3109	0.3993	0.2644	0.2164	0.4562	0.3118	0.2738
Graph-Flashback	0.4173	0.2925	0.2578	0.5548	0.3647	0.3154	0.4068	0.2648	0.2231	0.4645	0.3197	0.2765
STRelay+STGN	0.4316	0.2921	0.2576	0.5569	0.3709	0.3232	0.3748	0.2350	0.2024	0.4633	0.3076	0.2669
STRelay+Flashback	0.4473	0.3072	0.2721	0.5743	0.3859	0.3377	0.3978	0.2523	0.2175	0.4740	0.3177	0.2756
STRelay+SNPM	0.4484	0.3070	0.2723	0.5786	0.3837	0.3329	0.4172	0.2663	0.2259	0.4944	0.3258	0.2877
STRelay+Graph-Flashback	<b>0.4525</b>	<b>0.3101</b>	<b>0.2743</b>	<b>0.5835</b>	<b>0.3862</b>	<b>0.3381</b>	<b>0.4251</b>	<b>0.2728</b>	<b>0.2338</b>	<b>0.4970</b>	<b>0.3360</b>	<b>0.2915</b>

**Evaluation Metrics.** We adopt three evaluation metrics commonly used in prior work: Mean Reciprocal Rank (MRR), average Accuracy@K (Acc@K), and Normalized Discounted Cumulative Gain@K (NDCG@K) to evaluate the performance. In our experiments, we adopt the commonly used values  $K = \{5, 10\}$ . Please refer to the Appendix for the details of the metrics.

### Overall Performance Comparison

Table 2 shows the overall performance on all four datasets (due to limited space, we report the results of Acc@5 and NDCG@5 in Section Additional Results on Overall Performance Comparison in the Appendix), and we highlight the best-performing result on each task and for each dataset. We observe that STRelay+Graph-Flashback consistently outperforms all baselines, achieving 4.89%-8.47% improvement on average over the best-performing baselines across four datasets. Moreover, DeepMove, STAN and GETNext consider future temporal information but still yield suboptimal performance compared to STRelay enhanced baselines.

Notably, we observe that our STRelay framework consistently improves the location prediction performance of the corresponding base prediction methods STGN, Flashback, SNPM, and Graph-Flashback on all datasets, which demonstrates the universal effectiveness of STRelay. STRelay boosts the performance of the above four baselines with an average improvement of 3.19%-11.56% across different datasets in predicting the next location.

### Ablation Study

We consider three variants to quantify their impact on location prediction performance and demonstrate their utility. 1) *w/o spatial* is a variant that only considers future temporal contexts for location prediction. 2) *w/o temporal* is a variant that only considers future spatial contexts for location prediction. 3) *w/o relaying* is a variant that models future temporal and spatial contexts not in a relaying, but in a parallel manner.

The results are shown in Table 3. First, the complete STRelay framework significantly outperforms both the

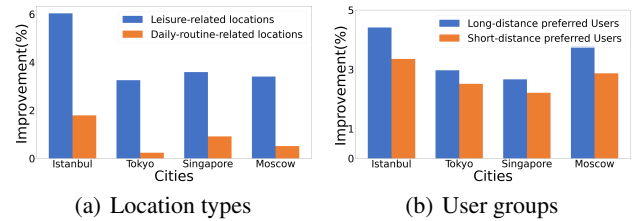


Figure 4: Performance improvement on different location types and user groups

spatial-ablated variant (*w/o spatial*) and temporal-ablated variant (*w/o temporal*) by 2.89% and 2.51% on average across four base models and four datasets, respectively, highlighting the essential contributions of modeling both temporal and spatial context. Moreover, we notice that the complete STRelay framework outperforms the *w/o relaying* variant by 1.49%-2.92% performance improvement across four base models and datasets, which demonstrates that our learning in a relaying manner indeed boosts performance by flexibly capturing the inherent relationship between temporal and spatial contexts. Note that due to limited space, we report the results of Acc@5 and NDCG@5 in Section Additional Results on Ablation Study in the Appendix.

### Performance Improvement Analysis on Location Types and User Groups

In this section, we investigate the performance improvement across different location types and user groups using STRelay with Graph-Flashback (the best-performing base model).

First, to study the performance improvement across different location types, we classify locations into corresponding activity categories following previous work (Yang et al. 2019). Specifically, we adopt a binary classification scheme consisting of: leisure-related locations (e.g., Outdoors and Entertainment) and daily-routine-related locations (e.g., College and Residence). Figure 4(a) shows the results of the percentage of performance improvement of Acc@10 in predicting these two types of locations on the

Table 3: Ablation Study

	Istanbul			Tokyo			Singapore			Moscow		
Methods	Acc@10	NDCG@10	MRR	Acc@10	NDCG@10	MRR	Acc@10	NDCG@10	MRR	Acc@10	NDCG@10	MRR
STRelay+STGN	<b>0.4316</b>	<b>0.2921</b>	<b>0.2576</b>	<b>0.5569</b>	<b>0.3709</b>	<b>0.3232</b>	<b>0.3748</b>	<b>0.2347</b>	<b>0.2024</b>	<b>0.4633</b>	<b>0.3076</b>	<b>0.2669</b>
<i>w/o spatial</i>	0.4050	0.2790	0.2491	0.5373	0.3599	0.3138	0.3597	0.2286	0.1980	0.4361	0.2901	0.2517
<i>w/o temporal</i>	0.4013	0.2763	0.2468	0.5381	0.3609	0.3148	0.3550	0.2258	0.1958	0.4443	0.2966	0.2574
<i>w/o relaying</i>	0.4095	0.2819	0.2515	0.5437	0.3633	0.3161	0.3659	0.2330	0.2017	0.4420	0.2948	0.2562
STRelay+Flashback	<b>0.4473</b>	<b>0.3073</b>	<b>0.2721</b>	<b>0.5743</b>	<b>0.3859</b>	<b>0.3377</b>	<b>0.3978</b>	<b>0.2523</b>	<b>0.2175</b>	<b>0.4861</b>	<b>0.3251</b>	<b>0.2816</b>
<i>w/o spatial</i>	0.4340	0.2999	0.2668	0.5559	0.3672	0.3171	0.3902	0.2491	0.2155	0.4688	0.3137	0.2723
<i>w/o temporal</i>	0.4366	0.3012	0.2677	0.5586	0.3695	0.3194	0.3939	0.2508	0.2167	0.4764	0.3212	0.2794
<i>w/o relaying</i>	0.4404	0.3029	0.2688	0.5651	0.3807	0.3316	0.3942	0.2511	0.2173	0.4707	0.3156	0.2740
STRelay+SNPM	<b>0.4484</b>	<b>0.3070</b>	<b>0.2723</b>	<b>0.5786</b>	<b>0.3837</b>	<b>0.3329</b>	<b>0.4172</b>	<b>0.2663</b>	<b>0.2259</b>	<b>0.4944</b>	<b>0.3258</b>	<b>0.2877</b>
<i>w/o spatial</i>	0.4364	0.3011	0.2677	0.5695	0.3781	0.3271	0.4040	0.2543	0.2185	0.4827	0.3270	0.2851
<i>w/o temporal</i>	0.4402	0.3032	0.2691	0.5715	0.3747	0.3222	0.4115	0.2575	0.2206	0.4877	0.3284	0.2853
<i>w/o relaying</i>	0.4403	0.3018	0.2674	0.5806	0.3851	0.3327	0.4015	0.2536	0.2182	0.4899	0.3286	0.2859
STRelay+Graph-Flashback	<b>0.4525</b>	<b>0.3101</b>	<b>0.2743</b>	<b>0.5835</b>	<b>0.3862</b>	<b>0.3381</b>	<b>0.4251</b>	<b>0.2728</b>	<b>0.2338</b>	<b>0.4993</b>	<b>0.3360</b>	<b>0.2915</b>
<i>w/o spatial</i>	0.4432	0.3052	0.2709	0.5763	0.3844	0.3333	0.4107	0.2594	0.2231	0.4934	0.3331	0.2898
<i>w/o temporal</i>	0.4453	0.3068	0.2723	0.5773	0.3805	0.3279	0.4110	0.2586	0.2220	0.4986	0.3349	0.2903
<i>w/o relaying</i>	0.4368	0.3009	0.2672	0.5741	0.3819	0.3305	0.4216	0.2685	0.2312	0.4827	0.3256	0.2832

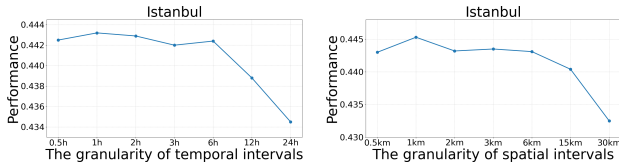


Figure 5: Impact of the granularity of temporal and spatial intervals on the Istanbul dataset

four datasets. We observe that the performance improvements stemming from leisure-related locations are consistently and significantly higher than those from daily-routine-related locations by 2.68%-4.25%, which demonstrates that modeling future spatiotemporal contexts is particularly beneficial for entertainment-related activities, which are more uncertain than daily-routine-related activities.

Second, we categorize users into two distinct groups based on their radius of gyration (Feng et al. 2020; Deng et al. 2025a), which is calculated as the root mean squared distance of all locations in a trajectory from the geographical center of the trajectory, and obtain two groups: long-distance preferred users (top 50%) and short-distance preferred users (bottom 50%). We report the performance improvements on these two user groups. As shown in Figure 4(b), both user groups exhibit performance improvements in Acc@10 across all four datasets, with long-distance preferred users consistently demonstrating larger improvement (0.45%-1.06% higher than short-distance preferred users). These results indicate that modeling future spatiotemporal contexts is more effective in capturing the mobility patterns of users who prefer traveling longer distances, which often implies higher uncertainty for next locations.

### Impact of Spatiotemporal Context Granularity

In this section, we use STRelay with Graph-Flashback to investigate the influence of the granularity of future temporal and spatial intervals on the performance (we report results

of Acc@10 here). Results are shown in Figure 5. Specifically, to investigate the impact of temporal interval granularity, we train the model with future time intervals ranging from 0.5 to 24 hours. We observe the performance decreases as temporal granularity becomes coarser, with 1h granularity achieving the best results. For spatial interval granularity, we use spatial intervals from 0.5 km to 30 km. The results show a similar trend, where performance drops as spatial granularity coarsens, with 1km granularity achieving the best results. Thus, we choose 1h and 1km as temporal and spatial granularities. (Similar trends are observed in the other three datasets; please refer to the Appendix for the results.)

## Conclusion

In this paper, we propose STRelay, a universal framework designed to explicitly model the future spatiotemporal contexts in a relaying manner; it can be flexibly integrated with different location prediction models to boost the prediction performance. Experimental results show that STRelay consistently boosts the performance of state-of-the-art baselines with an average improvement of 3.19%-11.56% across four datasets, demonstrating the universal effectiveness of STRelay. Moreover, we find that the future spatiotemporal contexts are particularly helpful for entertainment-related locations and also for user groups who prefer traveling longer distances. The performance gain on such non-daily-routine activities, which often suffer from higher uncertainty, is indeed complementary to the base location prediction models that excel at modeling regular daily routine patterns.

In the future, we plan to learn future spatiotemporal contexts using LLM to get better generalizability across cities.

## References

Cao, Y.; Li, A.; Lou, J.; Chen, M.; Zhang, X.; and Kang, B. 2021. An Attention-Based Bidirectional Gated Recurrent Unit Network for Location Prediction. In *2021 13th International Conference on Wireless Communications and Signal Processing (WCSP)*, 1–5. IEEE.

- Cheng, C.; Yang, H.; Lyu, M. R.; and King, I. 2013. Where you like to go next: Successive point-of-interest recommendation. In *IJCAI*.
- Deng, B.; Jing, X.; Yang, T.; Qu, B.; Yang, D.; and Cudre-Mauroux, P. 2025a. Revisiting synthetic human trajectories: Imitative generation and benchmarks beyond datasaurus. In *Proceedings of the 31st ACM SIGKDD Conference on Knowledge Discovery and Data Mining V. 1*, 201–212.
- Deng, B.; Qu, B.; Wang, P.; Yang, D.; Fankhauser, B.; and Cudre-Mauroux, P. 2025b. Replay: Modeling time-varying temporal regularities of human mobility for location prediction over sparse trajectories. *IEEE Transactions on Mobile Computing*.
- Feng, J.; Li, Y.; Zhang, C.; Sun, F.; Meng, F.; Guo, A.; and Jin, D. 2018. Deepmove: Predicting human mobility with attentional recurrent networks. In *Proceedings of the 2018 world wide web conference*, 1459–1468.
- Feng, J.; Yang, Z.; Xu, F.; Yu, H.; Wang, M.; and Li, Y. 2020. Learning to simulate human mobility. In *KDD*, 3426–3433.
- Feng, S.; Li, X.; Zeng, Y.; Cong, G.; Chee, Y. M.; and Yuan, Q. 2015. Personalized ranking metric embedding for next new POI recommendation. In *IJCAI*.
- Feng, S.; Meng, F.; Chen, L.; Shang, S.; and Ong, Y. S. 2024. Rotan: A rotation-based temporal attention network for time-specific next poi recommendation. In *Proceedings of the 30th ACM SIGKDD Conference on Knowledge Discovery and Data Mining*, 759–770.
- Gao, H.; Tang, J.; and Liu, H. 2012. Exploring social-historical ties on location-based social networks. In *Proceedings of the International AAAI Conference on Web and Social Media*, volume 6, 114–121.
- Li, X.; Hu, R.; Wang, Z.; and Yamasaki, T. 2021. Location Predicts You: Location Prediction via Bi-direction Speculation and Dual-level Association. In *IJCAI*, 529–536.
- Lian, D.; Wu, Y.; Ge, Y.; Xie, X.; and Chen, E. 2020. Geography-aware sequential location recommendation. In *Proceedings of the 26th ACM SIGKDD international conference on knowledge discovery & data mining*, 2009–2019.
- Liu, Q.; Wu, S.; Wang, L.; and Tan, T. 2016. Predicting the next location: A recurrent model with spatial and temporal contexts. In *AAAI*.
- Liu, X.; Yang, Y.; Xu, Y.; Yang, F.; Huang, Q.; and Wang, H. 2022. Real-time POI recommendation via modeling long- and short-term user preferences. *Neurocomputing*, 467: 454–464.
- Luo, Y.; Liu, Q.; and Liu, Z. 2021. Stan: Spatio-temporal attention network for next location recommendation. In *Proceedings of the web conference 2021*, 2177–2185.
- Ma, S.; Zheng, Y.; and Wolfson, O. 2013. T-share: A large-scale dynamic taxi ridesharing service. In *2013 IEEE 29th International Conference on Data Engineering (ICDE)*, 410–421. IEEE.
- Noulas, A.; Scellato, S.; Lathia, N.; and Mascolo, C. 2012. Mining user mobility features for next place prediction in location-based services. In *2012 IEEE 12th international conference on data mining*, 1038–1043. IEEE.
- Qin, Y.; Wu, H.; Ju, W.; Luo, X.; and Zhang, M. 2023. A diffusion model for poi recommendation. *ACM Transactions on Information Systems*, 42(2): 1–27.
- Rao, X.; Chen, L.; Liu, Y.; Shang, S.; Yao, B.; and Han, P. 2022. Graph-flashback network for next location recommendation. In *Proceedings of the 28th ACM SIGKDD conference on knowledge discovery and data mining*, 1463–1471.
- Rendle, S.; Freudenthaler, C.; Gantner, Z.; and Schmidt-Thieme, L. 2012. BPR: Bayesian personalized ranking from implicit feedback. *arXiv preprint arXiv:1205.2618*.
- Rendle, S.; Freudenthaler, C.; and Schmidt-Thieme, L. 2010. Factorizing personalized markov chains for next-basket recommendation. In *WWW*, 811–820. ACM.
- Song, C.; Ren, Z.; and Lu, L. 2025. Integrating personalized spatio-temporal clustering for next poi recommendation. In *Proceedings of the AAAI Conference on Artificial Intelligence*, volume 39, 12550–12558.
- Sun, K.; Qian, T.; Chen, T.; Liang, Y.; Nguyen, Q. V. H.; and Yin, H. 2020. Where to go next: Modeling long- and short-term user preferences for point-of-interest recommendation. In *Proceedings of the AAAI conference on artificial intelligence*, volume 34, 214–221.
- Sun, T.; Fu, K.; Huang, W.; Zhao, K.; Gong, Y.; and Chen, M. 2024. Going where, by whom, and at what time: Next location prediction considering user preference and temporal regularity. In *Proceedings of the 30th ACM SIGKDD Conference on Knowledge Discovery and Data Mining*, 2784–2793.
- Tang, J.; and Wang, K. 2018. Personalized top-n sequential recommendation via convolutional sequence embedding. In *Proceedings of the eleventh ACM international conference on web search and data mining*, 565–573.
- Vaswani, A.; Shazeer, N.; Parmar, N.; Uszkoreit, J.; Jones, L.; Gomez, A. N.; Kaiser, Ł.; and Polosukhin, I. 2017. Attention is all you need. *Advances in neural information processing systems*, 30.
- Wu, J.; Hu, R.; Li, D.; Ren, L.; Hu, W.; and Xiao, Y. 2022. Where have you been: Dual spatiotemporal-aware user mobility modeling for missing check-in POI identification. *Information Processing & Management*, 59(5): 103030.
- Xu, X.; Suzumura, T.; Yong, J.; Hanai, M.; Yang, C.; Kanezashi, H.; Jiang, R.; and Fukushima, S. 2023. Revisiting mobility modeling with graph: A graph transformer model for next point-of-interest recommendation. In *Proceedings of the 31st ACM international conference on advances in geographic information systems*, 1–10.
- Yang, D.; Fankhauser, B.; Rosso, P.; and Cudre-Mauroux, P. 2020. Location prediction over sparse user mobility traces using rnns. In *Proceedings of the twenty-ninth international joint conference on artificial intelligence*, 2184–2190.
- Yang, D.; Qu, B.; Yang, J.; and Cudre-Mauroux, P. 2019. Revisiting user mobility and social relationships in lbsns: a hypergraph embedding approach. In *WWW*, 2147–2157. ACM.



Yang, D.; Zhang, D.; Zheng, V. W.; and Yu, Z. 2014. Modeling user activity preference by leveraging user spatial temporal characteristics in LBSNs. *IEEE Transactions on Systems, Man, and Cybernetics: Systems*, 45(1): 129–142.

Yang, S.; Liu, J.; and Zhao, K. 2022. GETNext: trajectory flow map enhanced transformer for next POI recommendation. In *Proceedings of the 45th International ACM SIGIR Conference on research and development in information retrieval*, 1144–1153.

Yin, F.; Liu, Y.; Shen, Z.; Chen, L.; Shang, S.; and Han, P. 2023. Next POI recommendation with dynamic graph and explicit dependency. In *Proceedings of the AAAI conference on artificial intelligence*, volume 37, 4827–4834.

Yuan, Y.; Ding, J.; Wang, H.; Jin, D.; and Li, Y. 2022. Activity trajectory generation via modeling spatiotemporal dynamics. In *KDD*, 4752–4762.

Zhang, C.; Zhao, K.; and Chen, M. 2022. Beyond the limits of predictability in human mobility prediction: Context-transition predictability. *IEEE Transactions on Knowledge and Data Engineering*, 35(5): 4514–4526.

Zhao, P.; Luo, A.; Liu, Y.; Zhuang, F.; Xu, J.; Li, Z.; Sheng, V. S.; and Zhou, X. 2020. Where to go next: A spatio-temporal gated network for next poi recommendation. *IEEE Transactions on Knowledge and Data Engineering*.

Zhao, P.; Zhu, H.; Liu, Y.; Xu, J.; Li, Z.; Zhuang, F.; Sheng, V. S.; and Zhou, X. 2019. Where to go next: A spatio-temporal gated network for next POI recommendation. In *AAAI*, volume 33, 5877–5884.

Zhou, F.; Wang, P.; Xu, X.; Tai, W.; and Trajcevski, G. 2021. Contrastive trajectory learning for tour recommendation. *ACM Transactions on Intelligent Systems and Technology (TIST)*, 13(1): 1–25.

## Appendix

### Baselines

We choose the following models for location prediction as baselines: **BPR** (Rendle et al. 2012) learns user preferences on POIs by minimizing a pairwise ranking loss. **Caser** (Tang and Wang 2018) embeds POIs in user interaction history as images, using convolutional filters to capture both local and global sequential dependencies. **STGN** (Zhao et al. 2019): add additional gates controlled by the spatiotemporal distances between successive check-ins to LSTM, while **STGCN** (Zhao et al. 2019) is a variant of STGN with coupled input and forget gates for improved efficiency. Note that we add user preference modeling in our experiments for these two methods. **DeepMove** (Feng et al. 2018) adds an attention mechanism to GRU for location prediction over sparse mobility traces. **STAN** (Luo, Liu, and Liu 2021) Models relative spatial-temporal information among POIs with a bi-layer attention architecture. **GETNext** (Yang, Liu, and Zhao 2022) utilizes a global trajectory flow graph to enhance the prediction of the next POI, alongside proposing a GCN model for generating effective POI embeddings. **Flashback** (Yang et al. 2020) is an RNN-based framework that explicitly leverages high-order

spatiotemporal distance information to identify informative past hidden states. **SNPM** (Yin et al. 2023) represents POI relationships through knowledge graph embeddings and aggregates contextual information from neighboring nodes. **Graph-Flashback** (Rao et al. 2022) constructs a spatial-temporal knowledge graph for POI representation learning.

### The Details of Evaluation Metrics

In this section, we elaborate on the details of evaluation metrics. The definitions of Mean Reciprocal Rank (MRR), average Accuracy@K (Acc@K), and Normalized Discounted Cumulative Gain@K (NDCG@K) are as follows:

$$\text{MRR} = \frac{1}{m} \sum_{i=1}^m \frac{1}{\text{rank}_i} \quad (20)$$

where  $m$  is the number of predictions and the  $\text{rank}_i$  represents the rank of the true POI in the predicted ordered list. Acc@K is the rate of true positive samples in the predicted top- $K$  positive samples, which is computed as follows:

$$\text{Acc@K} = \frac{1}{|U|} \sum_{u \in U} \frac{|S_u^K \cap S_u^L|}{|S_u^K|}, \quad (21)$$

where  $S_u^K$  is the set of predicted top- $K$  POIs for user  $u$ ,  $S_u^L$  denotes the ground truth of user  $u$ . Unlike Acc@K, which focuses on top- $K$ , NDCG@K aims to measure the overall ranking performance of the model. The calculation formulation of NDCG@K is presented as follows:

$$\text{NDCG@K} = \frac{1}{|U|} \sum_{u \in U} \frac{1}{\log(\text{rank}_u + 1)} \quad (22)$$

where  $\text{rank}_u$  denotes the rank of  $S_u^L$  in  $S_u^K$  for user  $u$ . In our experiments, we adopt the commonly used  $K = \{5, 10\}$ .

### Experiment Settings

We developed our model using the PyTorch framework and conducted experiments on the following hardware platform (CPU: Intel(R) Xeon(R) Gold 5320, GPU: NVIDIA GeForce RTX 3090). We evaluate STRelay and the baselines in the location prediction task. We empirically set the dimension of hidden states and all (POI, timestamp, and user) embedding sizes as 10, and the temporal decay factor  $\alpha = 0.1$  and spatial decay factor  $\beta = 100$  on all datasets, and the sequence length is 20. All baseline implementations are either provided by the original authors or based on the original papers.

### Additional Results on Overall Performance Comparison

Table 4 shows the results of evaluation metrics Acc@5 and NDCG@5 overall location prediction performance comparison. We observe that STRelay+Graph-Flashback consistently outperforms all baselines, achieving 6.63% and 5.84% improvement on average over the best-performing baselines across four datasets on Acc@5 and NDCG@5, respectively. Additionally, our STRelay framework consistently enhances the performance of corresponding base prediction methods STGN, Flashback, SNPM, and Graph-Flashback with an average improvement of 2.54%-10.9% across four datasets.

Table 4: Additional results of location prediction performance

	Istanbul		Tokyo		Singapore		Moscow	
Methods	Acc@5	NDCG@5	Acc@5	NDCG@5	Acc@5	NDCG@5	Acc@5	NDCG@5
BPR	0.2532	0.1821	0.2133	0.1565	0.2077	0.1466	0.1362	0.0937
Caser	0.3179	0.2464	0.4115	0.2988	0.2392	0.1726	0.3239	0.2341
STGCN	0.3312	0.2514	0.4331	0.3104	0.2917	0.2102	0.3552	0.2587
DeepMove	0.2633	0.1903	0.4127	0.3020	0.2923	0.2053	0.2905	0.2035
STAN	0.2633	0.1903	0.4127	0.3020	0.2923	0.2053	0.2905	0.2035
GETNext	0.3107	0.2306	0.4214	0.3089	0.3171	0.2293	0.3528	0.2580
STGN	0.3292	0.2495	0.4415	0.3228	0.2736	0.1950	0.3475	0.2533
Flashback	0.3475	0.2632	0.4533	0.3339	0.2995	0.2159	0.3780	0.2802
SNPM	0.3458	0.2633	0.4538	0.3305	0.3138	0.2368	0.3913	0.2906
Graph-Flashback	0.3521	0.2711	0.4589	0.3346	0.3218	0.2376	0.3986	0.2967
STRelay+STGN	0.3604	0.2690	0.4625	0.3412	0.2914	0.2080	0.3841	0.2819
STRelay+Flashback	0.3779	0.2847	0.4803	0.3552	0.3116	0.2243	0.4009	0.2939
STRelay+SNPM	0.3781	0.2846	0.4801	0.3521	0.3279	0.2382	0.4167	0.3017
STRelay+Graph-Flashback	<b>0.3807</b>	<b>0.2873</b>	<b>0.4863</b>	<b>0.3555</b>	<b>0.3348</b>	<b>0.2433</b>	<b>0.4217</b>	<b>0.3113</b>

Table 5: Additional results of ablation study

	Istanbul		Tokyo		Singapore		Moscow	
Methods	Acc@5	NDCG@5	Acc@5	NDCG@5	Acc@5	NDCG@5	Acc@5	NDCG@5
STRelay+STGN	<b>0.3604</b>	<b>0.2690</b>	<b>0.4625</b>	<b>0.3412</b>	<b>0.2914</b>	<b>0.2081</b>	<b>0.3841</b>	<b>0.2819</b>
<i>w/o spatial</i>	0.3384	0.2574	0.4467	0.3304	0.2832	0.2039	0.3667	0.2675
<i>w/o temporal</i>	0.3344	0.2547	0.4475	0.3315	0.2793	0.2013	0.3756	0.2743
<i>w/o relaying</i>	0.3418	0.2599	0.4510	0.3332	0.2881	0.2079	0.3697	0.2713
STRelay+Flashback	<b>0.3779</b>	<b>0.2849</b>	<b>0.4803</b>	<b>0.3552</b>	<b>0.3116</b>	<b>0.2243</b>	<b>0.4092</b>	<b>0.3001</b>
<i>w/o spatial</i>	0.3670	0.2782	0.4587	0.3356	0.3075	0.2223	0.3941	0.2894
<i>w/o temporal</i>	0.3686	0.2792	0.4620	0.3381	0.3106	0.2238	0.4044	0.2977
<i>w/o relaying</i>	0.3726	0.2810	0.4728	0.3506	0.3092	0.2235	0.3965	0.2914
STRelay+SNPM	<b>0.3781</b>	<b>0.2846</b>	<b>0.4801</b>	<b>0.3521</b>	<b>0.3279</b>	<b>0.2382</b>	<b>0.4167</b>	0.3017
<i>w/o spatial</i>	0.3682	0.2790	0.4721	0.3464	0.3169	0.2261	0.4101	0.3034
<i>w/o temporal</i>	0.3719	0.2811	0.4710	0.3419	0.3199	0.2279	0.4137	<b>0.3043</b>
<i>w/o relaying</i>	0.3709	0.2793	0.4810	0.3526	0.3162	0.2259	0.4140	0.3039
STRelay+Graph-Flashback	<b>0.3807</b>	<b>0.2873</b>	<b>0.4863</b>	<b>0.3555</b>	<b>0.3348</b>	<b>0.2433</b>	0.4235	<b>0.3113</b>
<i>w/o spatial</i>	0.3737	0.2827	0.4784	0.3526	0.3202	0.2301	0.4180	0.3086
<i>w/o temporal</i>	0.3766	0.2845	0.4764	0.3477	0.3201	0.2292	<b>0.4241</b>	0.3105
<i>w/o</i>	0.3684	0.2787	0.4770	0.3503	0.3331	0.2399	0.4117	0.3025

## Additional Results on Ablation Study

Table 5 shows the ablation experiment results of evaluation metrics on Acc@5 and NDCG@5. First, the complete STRelay framework outperforms the spatial-ablated variant (*w/o spatial*) and temporal-ablated variant (*w/o temporal*) by 2.96% and 2.52% across four base models and datasets in most cases. Second, we observe that the complete STRelay framework outperforms the *w/o relaying* variant by 1.57%-2.86% performance improvement across four base models and datasets.

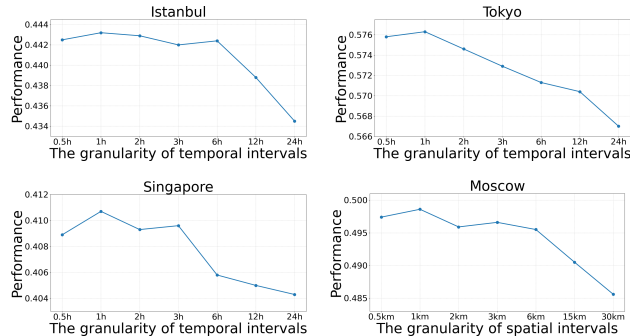


Figure 6: Impact of the granularity of temporal intervals

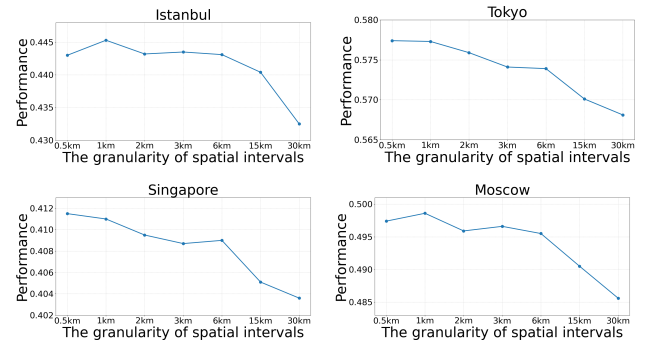


Figure 7: Impact of the granularity of spatial intervals

## Additional Results on Impact of Spatiotemporal Context Granularity

In this section, we use STRelay with Graph-Flashback as the base model to investigate the influence of the granularity of future temporal and spatial intervals.

Firstly, to investigate the impact of temporal context granularity, we train the model with future time intervals ranging from 0.5 to 24 hours. We report the results of Acc@10 on four datasets as shown in Figure 6. We observe a general trend where performance decreases as the temporal granularity becomes coarser. Besides, we find that the performance of the 1h granularity achieves the best results across

four datasets. Based on the above observations, we adopt 1h as the optimal temporal granularity.

Secondly, to investigate the impact of spatial context granularity, we train the model with spatial intervals ranging from 0.5 km to 30 km. The corresponding results of Acc@10 are presented in Figure 7. The results demonstrate the same overall trend observed for temporal granularity, where performance decreases as spatial granularity becomes coarser. Moreover, while the 1km spatial granularity yields slightly lower performance than 0.5km in the Singapore and Tokyo datasets, it achieves optimal performance in the Istanbul and Moscow datasets; thus, we adopt 1km as our spatial granularity in our experiment.